

3D Wing Model Analysis for Flutter Active Control

Eliza Munteanu*

*Advanced Studies and Research Center, 020042 Bucharest, ROMANIA (e-mail: eliza.munteanu@asrc.ro)

Abstract: The paper presents a possible way to obtain a numerical model for structural vibration active control. Using data and analysis results from different commercial software tools, such as ANSYS, ZAERO and MATLAB, one can find an optimal model to test the system dynamic response and design an active control law. Different algorithms for resolving the eigenvalue problem and different methods for system order reduction are presented here. A wing composite model as a representative aerospace structure is design and numerical tested for flutter.

Keywords: aerospace, flutter active control, composite structure.

1. INTRODUCTION

The aeroelastic phenomenon named flutter is usually the worst situation in real flight conditions. Numerical tests of a computational model are the first step in any flutter analysis. Large scale models with thousands of DOF are always a problem for engineers. In most applications, the main problem is to limit the modeling uncertainties and to reduce the system's order so that you not loose important effects on the model dynamics. Each particular case needs experimental system identification in order to validate the numerical model accuracy.

In order to obtain a complete numerical aeroservoelastic model some authors used a minimum-states formulation for the unsteady aerodynamic loads by resorting to balanced truncation techniques to reduce the dimension of an initial high order model [Bianchin et. al. (2003)]. A work presents a systematic guideline for the use of piezoelectric stack and monolithic patch smart materials in intelligent structures using the finite element method. Analytical, numerical, and experimental results are employed to verify the performance of piezoelectric stacks and patches as well as to determine the natural frequencies of typical strut and panel structures. These intelligent structures are employed to develop an actuator optimum voltage for active vibration suppression using modal, harmonic, and transient finite element analyses for a range of frequency encompassing a natural frequency [Ghasemi-Nejha et. al. (2006)]. A performance criterion is proposed for the optimization of piezoelectric patch actuator locations on flexible plate structures based on maximizing the controllability grammian [Peng et. al. (2005)]. This is followed by the determination of parameters required for actuator location optimization through Structuring Analysis in ANSYS Finite Element Analysis Package. Genetic Algorithm is then used to implement the optimization. Finally, with the actuators bonded on optimized locations, a filtered-x LMS-based multichannel adaptive control is applied to suppress vibration response of the plate. Other study presents a novel approach to optimizing the configuration of piezoelectric actuators for vibration control

of a flexible aircraft fin. The cost function for optimization using a genetic algorithm is derived directly from the frequency response function (FRF) obtained from a finite element model of the fin. In comparison to existing approaches, this method allows optimization on much more complex geometries where the derivation of an analytical cost function is prohibitive or impossible. The optimization approach is verified against experimental results obtained from a set of 12 actuators fixed to an experimental model of the fin [Rader et. al. (2007)]. One of paper presents the design of optimal constant gain output feedback based controllers for a nonlinear aeroelastic system. Controllers are designed for various sensor placements. For optimal sensor placement and with knowledge of the disturbance, the constant gain output feedback controller performance and robustness was found to be equivalent to that of linear quadratic regulator and linear quadratic Gaussian controllers for the example considered [Patil and Hodges (2002)]. The major objective of a paper is to describe a general methodology to design control laws in the context of a computational aeroelasticity environment [Dumitrache (2007)]. The technical approach involves employing a systems identification technique to develop an explicit state-space model for control law design from the output of a computational aeroelasticity code. The standard Linear Quadratic Gaussian (LQG) technique is employed and the computational aeroelasticity code is modified to accept control laws and perform closed-loop simulations. Numerical results for flutter suppression of the Benchmark Active Control Technology wind-tunnel model are given to illustrate the approach. A work focuses on the development of a design methodology for optimized flutter control of an aeroelastic delta wing. The approach rests on two main premises. The first is that the application of linear modelling and control design techniques can be used to control the predominantly nonlinear phenomenon of flutter by preventing its onset. The second lies in the spatial optimization of actuator and sensor parameters to facilitate control of targeted modes while providing roll-off of higher order modes without the need for phase-inducing filters [Richard and Clark (2003)]. Many papers in the flutter active control field does not present the

authors work in order to obtain the numerical model. Other kind of papers develops different specialized techniques for optimal placement of sensors/actuators, or for model order reduction in the case of control systems. On the other side, using some dedicated software without analyzing their capacity to simulate each particular physical problem, can lead to erroneous results. The present work tries to simplify and then validate the main steps of obtaining a flutter active control model by comparing different techniques results.

2. FE MODEL DESIGN AND ANALYSIS

A powerful and useful tool for vibration analysis is the ANSYS software.

In the present case, a model wing with an *Eppler 211* airfoil and basic dimensions semi-span - 650 mm and chord - 200 mm, was considered. The wing skin is built on composite material E-glass texture/orto-ophthalmic resin with 5 layers and 0.14 mm thickness each of them. The wing spars, placed at 30 %, respectively, 65 % of chord, are performed of the same material. In order to implement an active control law, two pairs of MFC (Macro Fiber Composite) actuators were glued on the wing skin (Fig.1). *Shell 99* elements with 6 DOF per node were chosen to predict the composite material behavior. A total of 2832 DOF were obtained, which means that the model can have 2832 natural modes in a modal analysis. In fact, the *Block Lanczos* algorithm for extracting the model eigenvalues, the most accuracy and faster ANSYS solver, allows calculating all natural frequencies lower than 1 MHz. The *Block Lanczos* algorithm uses the subspace eigenvalue method and is a variation of the classical *Lanczos* algorithm, where the *Lanczos* recursions are performed using a block of vectors, as opposed to a single vector [ANSYS Release]. Using this algorithm, only 1395 natural frequencies were found between 21.86 and, respectively 9.19×10^5 Hz. It remind the equation for undamped modal analysis

$$M\ddot{q} + Kq = 0 \tag{1}$$

where *M* and *K* are the mass and, respectively, the stiffness matrices.

The ANSYS modal analysis also allows printing out the mass and the stiffness matrices in a *Harwell Boeing* sparse matrix file format. A MATLAB routine can be develop to read from this file the two matrices in the MATLAB sparse format.

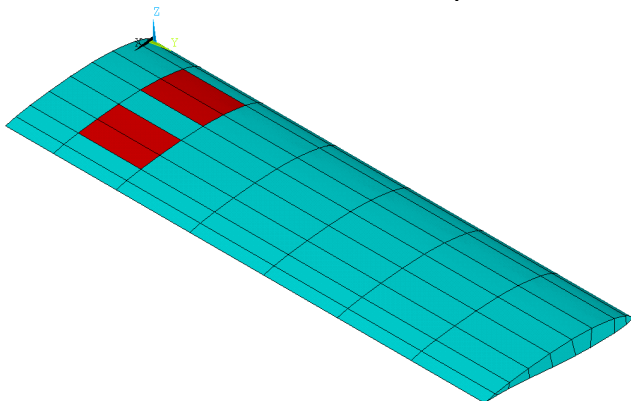


Fig. 1. The ANSYS wing model with the two pairs of MFC actuators.

Two MATLAB functions to compute the eigenvalues were tested: *eigs* and *sptarn* [http://www.mathworks.com]. Both of them use *Arnoldi* algorithm to extract a few eigenvalues. *Eigs* function allowed calculating the first 500 natural frequencies and the corresponding eigenvectors with very small errors. By comparison, the *sptarn* function founded all the 1395 frequencies with very small errors, but the eigenvectors are ordered so that

$$\text{norm}(M \times V - K \times V \times \text{diag}(lmb)) \tag{2}$$

is small. In (2) *V* is the modal matrix and *lmb* are the eigenvalues of the system. More than that, in the case of *sptarn* function, the convergence is very slow and the solution must be search in many defined domain of eigenvalues.

In Table 1 are presented the first 10 estimated natural frequencies for each method. The first column shows the ANSYS results, the second are the frequencies founded with *eigs* function, the third are frequencies calculated with the reduced mass and stiffness (obtained from *eigs*), and, finally it have the results of the *sptarn* function. One can observe that all the algorithms give the same results in the low natural frequencies domain. For the first 500 structural modes, the maximum difference between the results of the two MATLAB functions is 1.8344×10^{-6} Hz. On the other hand, the maximum difference between the MATLAB and ANSYS results are 0.499 Hz (Fig. 2). In this graphic of errors evolution can be observed 3 stages of precision: for the first 20 modes the errors are less than 0.05 Hz, between the 20th and the 200th modes the errors are less than 0.1 Hz, respectively, between the 200th and the 500th modes the errors grow up to 0.5 Hz. Usually, in vibration structural analysis no more than first 20 modes are examined, so it can conclude that in the low frequencies domain the MATLAB results are very accurate. In order to obtain the equation of system's dynamic in state space it need to move the problem from the physical coordinates in modal coordinates.

$$V^T M V \ddot{q} + V^T K V q = 0 \tag{3}$$

This implies that the modal matrix is needed. Because the *eigs* function generates this matrix, a first system order reduction eliminates the structural modes with frequencies higher than 30 KHz.

Table 1. Natural frequencies obtained with different algorithms

ANSYS	<i>eigs</i>	calculated from <i>M</i> and <i>K</i>	<i>sptarn</i>
21.8560	21.8556	21.8556	21.8556
117.5500	117.5548	117.5548	117.5548
131.8600	131.8579	131.8579	131.8579
156.0500	156.0489	156.0489	156.0489
337.5100	337.5057	337.5057	337.5057
442.1300	442.1342	442.1342	442.1342
573.2200	573.2150	573.2150	573.2150
692.3400	692.3418	692.3418	692.3418
724.1000	724.0969	724.0969	724.0969
813.2400	813.2394	813.2394	813.2394

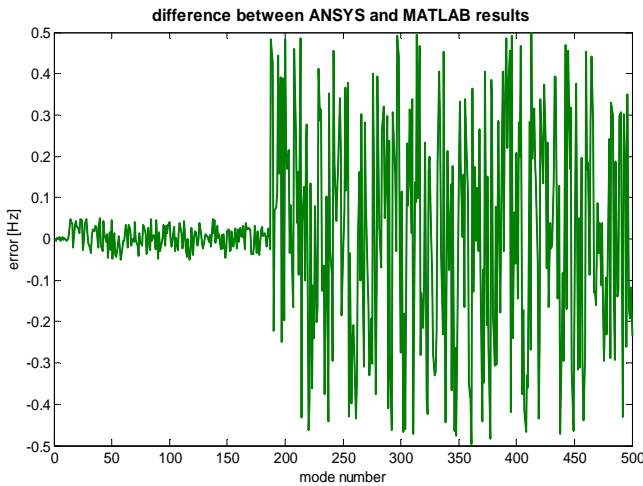


Fig. 2. Errors evolution between ANSYS and MATLAB results.

3. THE PLACEMENT OF ACTUATORS AND SENSORS

Many researchers developed some optimal placement techniques. Two usual approaches are used: minimizing the control energy required by maximizing a measure of the controllability Gramian matrix, and maximizing the control force [Bruant and Proslie (2005)].

In the present case it was tried to obtain the maximum force given by the actuators. The actuators are two pairs of MFC and for exciting the structure can be use an electromagnetic shaker. Two accelerometers with the possibility to measure the vertical displacement (z axis) will be considered as sensors. As point of applying the perturbation had been chosen two possible locations at $1/3$ from the leading edge of every wing sections: to the free end of the wing and, respectively, at $2/3$ from the clamped end of the wing. Static analyses in ANSYS were ruled. A unit static force was applied in these 2 points and, in both case, the maximum displacement on z axis appeared on the tip of the wing. It can conclude that the sensors will be placed on the tip of the wing. Because they must give information in the case of some torsional or coupled modes, one of them it will be at the leading edge and the other one at the trailing edge of the wing section.

For the actuators placement the system step response can be studied. For this step it must be obtained the state space equation of the system and the equation of measurement output by using the ANSYS static analysis results. *Shell 99* elements from ANSYS does not provide piezoelectric degree of freedom, but it can be approximated that the thermal strain obtained by applying a unit temperature on the actuators surface it is similar with the piezoelectric strain obtained by applying 1V. This thermal analogy was used by many authors [Mechbal (2005)] with good results. As location were tested 3 variants: at the root, in the middle and at the tip of the wing. Assuming the static interaction cause-effect

$$Kq_k = B_2 u_k, Kq_k = B_1 \xi_k \tag{4}$$

where B_2 represents the matrix of the control influence and q_k is the displacement vector corresponding to a unitary electric field u_k applied to the k MFC actuator, it can be determined the B_2 matrix. Similarly, by applying a unitary force can be obtained the vector of the perturbation influence B_1 . In physical coordinates the dynamic equation of system is

$$M\ddot{x} + Kx = B_2 u + B_1 \xi \tag{5}$$

and using the modal matrix V calculated with *eigs* function, the relation (4) become (in modal coordinates)

$$M + \text{diag}(\omega_i^2) x = \bar{B}_2 u + \bar{B}_1 \xi \tag{6}$$

where $\bar{B}_2 = V^T B_2, \bar{B}_1 = V^T B_1$. In terms of first order state form system that means

$$\begin{aligned} \dot{x}(t) &= Ax(t) + B_2 u(t) \\ y(t) &= C_2 x(t) \end{aligned} \tag{7}$$

where $y(t)$ is the measured output and C_2 include the influence of the z axis displacement for the nodes where the sensors are positioned. Two Matlab functions were tested: *step* and *lsim* for the system step response. In fig. 3 and fig. 4 similar results for both cases can be noticed. It seems that the second variant of placement, when the actuators are in the middle position (fig. 5), is the optimal location in order to obtain the maximum amplitude of the wing free end. Comparing the influence of each pair of actuators it can be stated that the actuators from the leading edge are more efficient, but the difference is small. The same behaviour has been observed regarding the sensors: the signal received from the leading edge sensor is a little stronger than the signal from the other sensor.

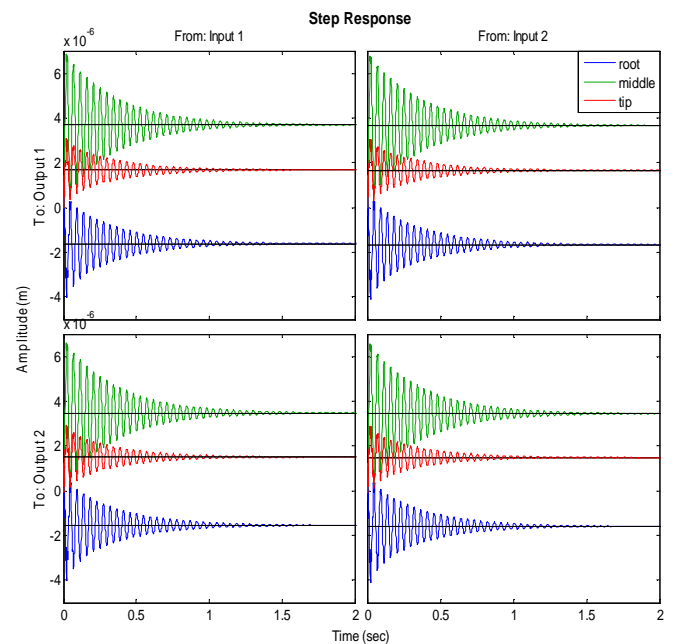


Fig. 3. Step response of the system in three cases of actuators placement obtained by using *step* function.

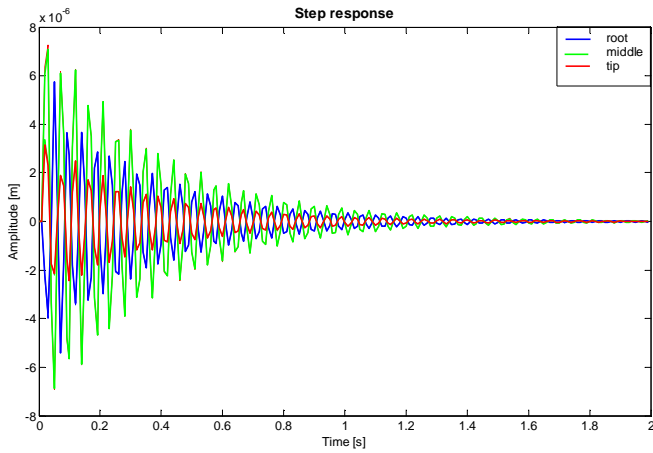


Fig. 4. Step response of the system in three cases of actuators placement obtained by using *lsim* function.

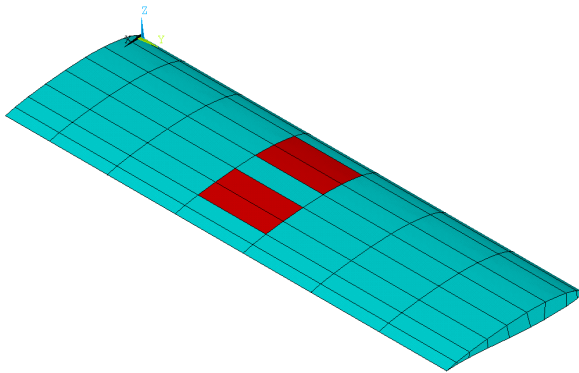


Fig. 5. The optimal location for the actuators.

Table 2. Actuators placement influence

Actuators placement on the wing span	Input 1 to output 1 <i>svd</i> × 10 ⁻⁶	Input 1 to output 2 <i>svd</i> × 10 ⁻⁶	Input 2 to output 1 <i>svd</i> × 10 ⁻⁶	Input 2 to output 2 <i>svd</i> × 10 ⁻⁶
Root	0.4681	0.4678	0.4786	0.4782
Middle	0.7404	0.7374	0.7348	0.7318
Tip	0.2865	0.2860	0.2840	0.2835

Quantitative results from each placement are presented in Table 2, where *input 1* and *output 1* represent the pair of actuators, respectively the sensor from the leading edge.

4. MODEL ORDER REDUCTION

The control laws are usually designed for structures with small number of degrees of freedom (DOF), so it must be found a way to reduce the modeled system order, with thousands of DOF, to a similar system with no more than 10 DOF for example. There is no efficient solution for this problem, as all the methods involve compromise approaches [Megretski (2004)]. It is well known that, regarding the energy introduced in system, the high frequency modes do not have significant influence on the system dynamics. So, a simple way to reduce the system order is to eliminate these high frequency modes, method that it already applied in this work (modal truncation). An other technique uses so called Guyan reduction based on the selection of DOF where the

force is applied and where the sensor is located. This method can not be followed in the case of MIMO systems, in which case an alternative is to eliminate those modes that are not controllable and observable. A measure of the controllability and observability degree is the controllability/observability grammian defined as

$$W_C^2 = \int_0^\infty e^{At} B_2 B_2^T e^{A^T t} dt \tag{8}$$

$$W_O^2 = \int_0^\infty e^{A^T t} C_2^T C_2 e^{At} dt$$

These grammians characterize the degree of controllability and observability by quantifying how far away from being singular the matrices of controllability and observability are. In other words it needs to quantify the rank deficiency and a possible way is to examine the singular values of the matrix [Inman (2006)]. For a stable system Hankel singular values indicate the respective state energy of the system. Hence, reduced order can be directly determined by examining the system Hankel SV's. The singular values of a stable system are defined as

$$\sigma_H = \sqrt{\lambda_i W_O W_C} \tag{9}$$

The MATLAB Robust Control Toolbox offers several algorithms for model approximation and order reduction. Robust control theory quantifies a system uncertainty as either additive or multiplicative types. These algorithms let control the absolute or relative approximation error, and are all based on the Hankel singular values of the system. In a first step, it can plot the Hankel SV of the full order system and choose the retained system order in view of reduction (Fig. 6). It is obviously that the first mode had the main contribution, so a 20th order system can be considered adequately for the next analysis. The obtained results of five model order reduction algorithms (Square-root balanced model truncation “balance”, Schur balanced model truncation “Schur”, Hankel minimum degree approximation “Hankel”, Balanced stochastic truncation “BST” and Normalized coprime balanced truncation “NCF”) are similar. The retained system frequencies are in almost all the cases (excepting Hankel minimum degree approximation): 21.86, 132.43, 156.94, 1756.16, 2401.52, 5708.54, 8546.60, 11516.84, 12378.48, respectively 14538.78 Hz, which means the frequencies of the mode number: 1, 3 and 4 for sure.

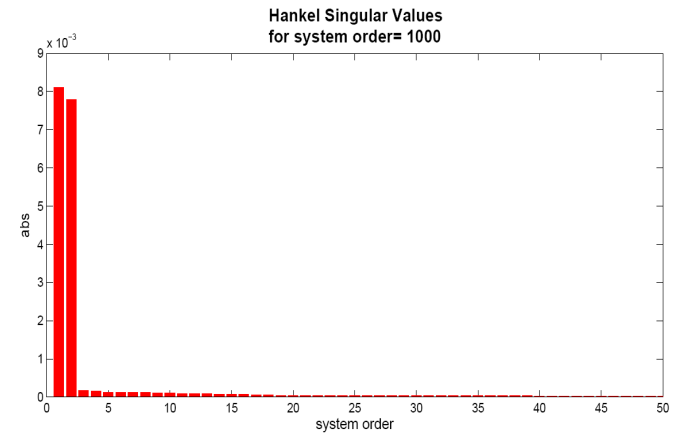


Fig. 6. Hankel SV of the full order system.

Upwards to the fourth mode, the reduced system frequencies are not exactly the same with the full order system or the FE model and the next mode can be the 20th or 21st. A first conclusion is that from point of view of the control law the first four modes are controllable and observable. Because it do not know how these structural modes are coupled with the aerodynamic modes, can be useful to obtain a reduced system which contains at least the first ten structural modes. So, in a next step a modal truncation of the full order system is performed by selecting those rows and columns from the system matrices which correspond to the first ten modes. The L_∞ norm can be a measure of how far away from the full system is the reduced system. In table 3 these norms for the six reduced systems are presented: balance, Schur, Hankel, BST, NCF and modal truncation. It notices that the norm value in the case of modal truncation reduction is larger than the others. The rank calculation of controllability and observability matrices confirm that only three from ten modes (six states) are full controllable/observable in the modal truncation reduced system. A conclusion of this section is that the control law must be design on the modes number 1, 3 and 4, all the superior modes that are controllable/observable having too high frequencies for a structural control case. The comparison of the L_∞ norm for different reduction algorithms and the advantage of diagonal form for system matrices (which allows analyzing every mode behavior) lead to choose a modal truncation reduction. An aeroelastic analysis will determine which of the first ten modes will be retained.

5. FLUTTER ANALYSIS

The aerodynamic flows also possess a modal character. The aeroelastic modes are those that exist when the structural and the aerodynamic modes are fully coupled, for example when oscillations of a fluid mode excite all structural modes and vice versa [Dowell (2004)]. The fluid-structure interaction of structural, inertial and aerodynamic forces may lead for a structure to become unstable or “flutter”. Flutter is just dynamic, rapidly developed, oscillatory instability of a non-rigid wing that occurs, at the flutter speed. Near this speed the fluid and structural modes become strongly coupled.

A dedicated software for solving the aeroelasticity problems is the code ZAERO. The ZAERO flutter module contains two flutter solution techniques: the K -method and the g -method. The g method is a newly developed flutter solution method that generalizes the K -method and the P - K method for true damping prediction. It is shown that the P - K method is only valid at the conditions of zero damping, zero frequency, or linearly varying generalized aerodynamic forces (Q_{ij}) with respect to reduced frequency. In fact, if Q_{ij} is highly nonlinear, it is shown that the P - K method may produce unrealistic roots due to its inconsistent formulation. The flutter module has a built-in atmospheric table as an option to perform matched-point flutter analysis. Sensitivity analysis with respect to the structural parameters is also included in the g -method [<http://www.zonatech.com>]. The first step for ZAERO flutter analysis is to create an external file with modal data from ANSYS. This file contains the nodes coordinates and the modal solutions for each structural mode.

ZAERO read the file to calculate the mass and stiffness matrices, to interconnect the structural elements with the aerodynamic grid and so on. The structural modal damping is selected to 2% for each mode. The next step is to define the airflow condition: freestream Mach number 0.6, symmetric boundary conditions, density (1.25 kg/m³); it must be defined the chord, semispan and wing area (identically with the FE model), respectively the position for aerodynamic center. Next, the panels for generalized aerodynamic forces calculus are chosen by defining the number of chord/span divisions, length of the tip and the root wing chord, leading edge radius at the root/tip normalized by the root/tip chord. It also need to specify values for the camber of the airfoil at the wing root/tip and the half thickness at the wing root/tip. The matrices of aerodynamic influence coefficients can be stored in an external file in order not to be calculated on every run of the program. A linear method for unsteady subsonic aerodynamics (ZONA6) is selected, method with higher-order panel formulation for lifting surfaces than the Doublet Lattice Method (DLM). The spline function establishes the displacement/force transferral between the structural Finite Element Method (FEM) model and the ZAERO aerodynamic model. An Infinite Plate Spline method that jointly assembles the spline matrix is chosen. Four possible flutter modes are obtained for a maximum speed of 800 m/s (Table 4). Table 5 presents each structural mode contributions for every flutter mode. The first flutter mode appear at 276.94 m/s with a reduced frequency of 78.85 Hz and the fourth structural mode has the main contribution on this flutter mode. So, the fourth structural mode is the first mode that can lead to a wing flutter. The same structural mode has the main contribution on the third and fourth flutter modes (aeroelastic modes which are caused by two aerodynamic lags).

Table 4. Flutter modes

	Speed [m/s]	Reduced frequency [Hz]	Dynamic pressure [kg/m/s ²]
Flutter mode 1	276.94	78.85	4.6976E+04
Flutter mode 2	620.95	352.26	2.3617E+05
Flutter mode 3	500.02	0.00	1.5314E+05
Flutter mode 4	390.63	0.00	9.3464E+04

Table 5. Structural modes participation to flutter modes

Structural modes	Flutter mode 1 partition [%]	Flutter mode 2 partition [%]	Flutter mode 3 partition [%]	Flutter mode 4 partition [%]
Mode 1	7.7041	13.5306	20.0251	20.0272
Mode 2	6.3594	13.3624	0.0170	0.0085
Mode 3	3.7219	5.4648	10.8106	10.8080
Mode 4	100.00	13.3467	100.00	100.00
Mode 5	6.3802	30.8081	0.0142	0.0228
Mode 6	6.1950	100.00	0.3321	0.3408
Mode 7	6.3539	13.1229	0.0635	0.0551
Mode 8	6.3496	13.9298	0.0443	0.0358
Mode 9	6.3499	13.5695	0.0388	0.0303
Mode 10	6.3489	16.2153	0.0238	0.0153

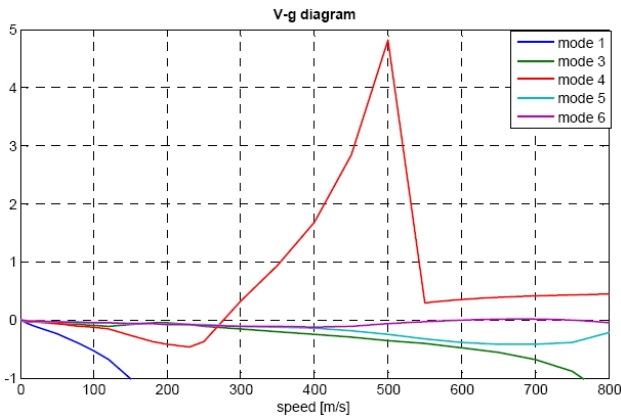


Fig. 7. Speed versus artificial damping diagram for the most important structural modes.

The next dangerous structural mode seems to be the sixth one; also, the first and the fifth structural modes have some significant contributions on some of the flutter modes. On the other hand it is clearly that the structural modes number 2, 3, 7, 8, 9 and 10 can not lead to flutter. Consequently, in the VG diagram it plot only the first, third, fourth, fifth and sixth modes behavior (Fig. 7).

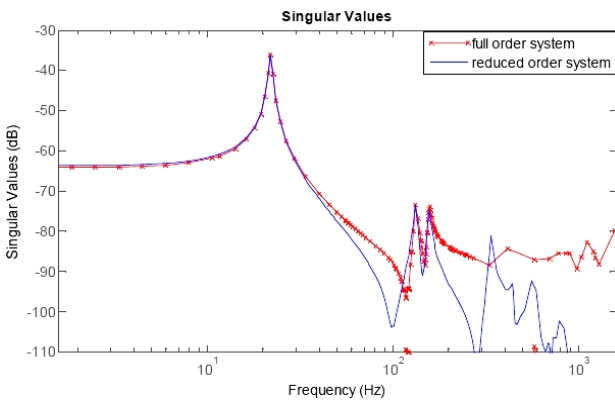


Fig. 8. Singular values for the full order and reduced order systems.

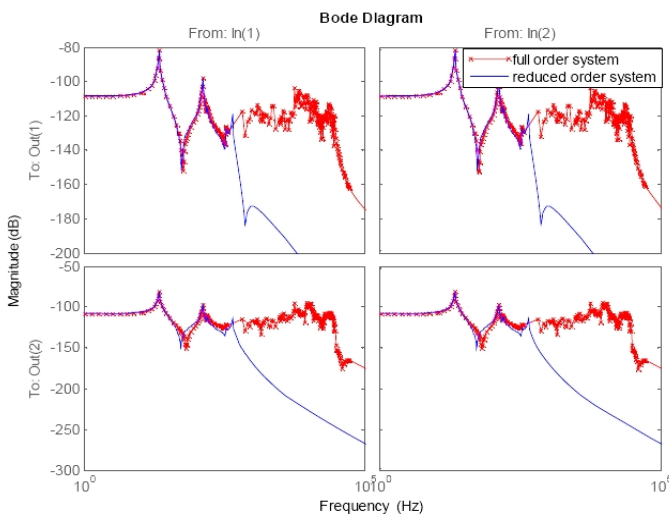


Fig. 9. Step response for the full order and reduced order systems.

For the same reason it can conclude that the control law must be designed for the first and the fourth structural modes (which are controllable and observable, as it already know), but the system matrices must contain, also, the third, fifth and sixth modes.

So, a final model order reduction will be a modal truncation from the system with the first ten modes to a reduced one which includes modes number 1, 3, 4, 5 and 6. From the full order system it retains only those lines and rows which correspond with these selected modes. A final analysis compares the singular values (fig. 8), the L_{∞} norm (3.3445e-004), respectively, the step response (fig. 9) of the full order and reduced order systems.

6. CONCLUSIONS

The present work tries to obtain a simplified model for flutter active control in comparison with other author’s research and publications [Rocha et al. (2007)]. Different techniques for optimal placement of sensors/actuators and model order reduction were analyzed and combined. Also, it has tried to take into account both the control system engineers and mechanical engineers concepts and approaches. Practical and software limitations approximate the obtained numerical model. A next presentation will design some active control laws to test this model, but only an experimental work can validate all. The intention is to use an extended Linear Quadratic Gaussian with Loop Transfer Recovery control law. In order to demonstrate the control performance and robustness to parametric uncertainties, the controller and the filter will be designed taking into account the selected modes, number 1, 3, 4, 5, respectively 6, but the system with all the first ten modes will be tested.

Respectfully thanks to Professor *Daniel J. Inman* from Virginia Tech for his advices and appreciation.

REFERENCES

ANSYS Release 11.0 Documentation for Ansys, Theory reference, Chapter 15. Analysis Tools, 15.16. Eigenvalue and Eigenvector Extraction.

Bianchin M., Quarantay G., Mantegazza P., State space reduced order models for static aeroelasticity and flight mechanics of flexible aircrafts, *Presented at the XVII Congresso Nazionale AIDAA*, 2003.

Bruant, I. and Proslie, L., Optimal Location of Actuators and Sensors in Active Vibration Control, *Journal of Intelligent Material Systems and Structures*, Vol.16, pp. 197-206, 2005.

Dowell, E.H. (Editor), A Modern Course in Aeroelasticity, *Kluwer Academic Publishers*, 2004.

Dumitrache, A., Active control laws for computational aeroelasticity, *2nd European Conference for Aerospace Sciences (EUCASS)*, 2007.

Ghasemi-Nejhad, M.N., Pourjalali S., Uyema M. and Yousefpour, A., Finite Element Method for Active Vibration Suppression of Smart Composite Structures using Piezoelectric Materials, *Journal of Thermoplastic Composite Materials*, Vol. 19; pp. 309-352, 2006.

- http://www.mathworks.com/access/helpdesk/help/techdoc/matlab_product_page.html
- <http://www.zonatech.com/Downloads.htm>, ZAERO Version 8.3 User's Manual, Zona Technology, Inc., 2008.
- Inman, D.J., *Vibration with Control*, John Wiley & Sons, Ltd., 2006.
- Mechbal, N., Simulations and experiments on active vibration control of a composite beam with integrated piezoceramics, *Proceedings of 17th IMACS World Congress*, 2005.
- Megretski, A., *Multivariable Control Systems, Lectures notes on Massachusetts Institute of Technology*, Department of Electrical Engineering and Computer Science, 2004.
- Patil, M.J. and Hodges, D.H., Output Feedback Control of the Nonlinear Aeroelastic Response of a Slender Wing, *Journal of Guidance, Control and Dynamics*, vol. 25, no. 2, pp. 302 – 308, 2002.
- Peng, F., Ng, A. and Hu, Y.-R., Actuator Placement Optimization and Adaptive Vibration Control of Plate Smart Structures, *Journal of Intelligent Material Systems and Structures*, Vol. 16, pp. 263-271, 2005.
- Rader, A.A., Afagh, F.F., Yousefi-Koma, A. and Zimcik, D.G., Optimization of Piezoelectric Actuator Configuration on a Flexible Fin for Vibration Control using Genetic Algorithms, *Journal of Intelligent Material Systems and Structures*, Vol. 18, pp.1015-1033, 2007.
- Richard, R.E. and Clark, R. L., Delta Wing Flutter Control Using Spatially Optimized Transducers, *Journal of Intelligent Material Systems and Structures*, Vol. 14, pp. 677- 691, 2003.
- Rocha, J., Moniz, P. and Suleman, A., Aeroelastic Control of a Wing with Active Skins Using Piezoelectric Patches, *Mechanics of Advanced Materials and Structures*, Vol.14, pp. 23-32, 2007.